Stereochemistry of the $[Ni_9(CO)_{18}]^{2-}$ Dianion: A Comparative Structural-Bonding Analysis of the Different Nine-Metal Cores of Stacked Metal Triangles in the $[M_9(CO)_{18}]^{2-}$ (M = Ni, Pt) and $[Rh_9(CO)_{19}]^{3-}$ Anions

Dick A. Nagaki,[1a] Loren D. Lower,[1a] Giuliano Longoni,[1b] Paolo Chini,[†1b] and Lawrence F. Dahl*[1a]

Department of Chemistry, University of Wisconsin—Madison, Madison, Wisconsin 53706, and the Istituto di Chimica Generale dell'Universita di Milano, 20133 Milano, Italy

Received February 14, 1986

The Longoni–Chini $[Ni_9(CO)_{18}]^{2-}$ dianion was obtained in essentially quantitative yield by oxidation of the trigonal-antiprismatic $[Ni_6(CO)_{12}]^{2-}$ dianion with $FeCl_3$. A single-crystal X-ray diffraction analysis of its $[AsPh_4]^+$ salt showed this dianion to consist of three stacked $Ni_3(CO)_3(\mu\text{-}CO)_3$ layers which are oriented such that the Ni_9 core possesses a heretofore unknown nine-vertex polyhedral conformation. The Ni_9 architecture, which closely conforms to C_3 symmetry, is best described as originating from a C_{3v} polyhedron formed by a trigonal antiprism and a trigonal prism sharing a common triangular face. An angular twisting deformation of the trigonal-antiprismatic Ni_6 fragment from a regular-staggered D_{3d} conformation gives rise to two groups of intertriangular Ni–Ni distances—viz., three shorter bonding ones of range 2.749 (3)–2.782 (3) Å, whose mean of 2.77 Å is identical with that for the six equivalent intertriangular Ni–Ni distances in the D_{3d} $[Ni_6(CO)_{12}]^{2-}$ dianion, and three longer, weakly bonding ones of range 2.876 (3)–2.989 (3) Å and mean 2.94 Å. An angular distortion of the trigonal-prismatic Ni_6 fragment from a regular eclipsed D_{3h} conformation results in three bonding intertriangular Ni–Ni distances of range 2.704 (3)–2.736 (3) Å and mean 2.72 Å. The nine intratriangular Ni–Ni distances of range 2.368 (3)–2.405 (3) Å and mean 2.39 Å agree well with the value of 2.38 Å for the six equivalent intratriangular Ni–Ni distances in the $[Ni_6(CO)_{12}]^{2-}$ dianion. The carbonyl ligands in both external $Ni_3(CO)_3(\mu\text{-}CO)_3$ layers are considerably bent out from their Ni_3 planes; the terminal and bridging carbonyl ligands of the interior $Ni_3(CO)_3(\mu\text{-}CO)_3$ layer are slightly bent out of the trinickel plane in opposite directions from each other. These geometrical features of the $[Ni_9(CO)_{18}]^{2-}$ dianion are presumed to be a consequence of a subtle interplay between electronic and steric effects. The idealized Ni_9 core is a geometrical hybrid of the face-sharing bi(trigonal-prismatic) D_{3h} polyhedron determined for the Pt_9 core in the $[Pt_9(CO)_{18}]^{2-}$ dianion and the face-sharing bi(trigonal-antiprismatic) or bioctahedral D_{3h} polyhedron found for the Rh_9 core in the $[Rh_9(CO)_{19}]^{3-}$ trianion. These three types of nonametal cores represent the three regular-stacked conformers which can be constructed from three superimposed equilateral metal triangles with different rotational sequences about the principal threefold axis. The observed stacking pattern for the Ni_9 core in the $[Ni_9(CO)_{18}]^{2-}$ dianion is in accordance with electronic considerations based upon the application of electron-counting schemes. In light of the results of recent theoretical calculations on the $[M_3(CO)_3(\mu\text{-}CO)_3]_n^{0,2-}$ monomers (n = 1) and dimers (n = 2) of nickel and platinum and the platinum trimer (n = 3), a qualitative bonding model is presented for the $[Ni_9(CO)_{18}]^{2-}$ dianion. $[AsPh_4]^+_2[Ni_9(CO)_{18}]^{2-}$: fw, 1799.17; monoclinic; $P2_1/n$; a = 20.347 (4) Å, b = 15.758 (5) Å, c = 22.820 (8) Å, β = 114.38 (2)°, V = 6663.8 Å^3; D(calcd) = 1.79 g/cm^3 for Z = 4. Anisotropic least-squares refinement converged at $R_1(F)$ = 8.49%, $R_2(F)$ = 7.01% for 4927 independent absorption-corrected data ($F > 3\sigma(F)$) obtained at room temperature via a refurbished Nicolet diffractometer with Mo Kα radiation.

Introduction

Syntheses and structural characterizations of the $[Pt_3(CO)_6]_n^{2-}$ dianions (n = 2–5) were initially reported[2,3] in 1974. This new series of inorganic oligomers was obtained by Longoni and Chini[2,3] either from the reduction of $Pt(CO)_2Cl_2$ with alkali metals in the presence of carbon monoxide or more conveniently from the reduction of sodium hexachloroplatinate(IV) with carbon monoxide and methanolic sodium hydroxide at atmospheric pressure and room temperature. X-ray crystallographic studies of the dianions (n = 2–5) by Calabrese, Lower, and Dahl[2,4] revealed a remarkable tendency for these Pt_{3n} clusters to adopt analogous (triangular metal)-stacking geometries based upon the oligomerization of n $Pt_3(CO)_3(\mu\text{-}CO)_3$ subunits by interlayer Pt–Pt bonding. Observed small rotational and translational displacements of these subunits in a given oligomer from an overall eclipsed D_{3h} conformation were attributed to carbonyl repulsions.

The synthesis and structural determination of the $[Ni_6(CO)_{12}]^{2-}$ dianion were also reported[5,6] in 1974. This red cluster was prepared by Chini, Longoni, and Martinengo[5,6] from the reduction of $Ni(CO)_4$ with either sodium metal in THF or potassium hydroxide in methanol. An X-ray diffraction study[5] showed a trigonal-antiprismatic D_{3d} geometry formed from two $Ni_3(CO)_3(\mu\text{-}CO)_3$ subunits in sharp contrast to the trigonal-prismatic D_{3h} geometry found for the $[Pt_6(CO)_{12}]^{2-}$ dianion.

In 1976 Longoni and Chini[7] reported the synthesis and chemical characterization of the $[Ni_9(CO)_{18}]^{2-}$ dianion (1), which was isolated as tetrasubstituted ammonium, phosphonium, and arsonium salts, either by a redox condensation between the $[Ni_6(CO)_{12}]^{2-}$ dianion and $Ni(CO)_4$ in THF solution or more conveniently by oxidation of the $[Ni_6(CO)_{12}]^{2-}$ dianion with nickel(II) chloride in EtOH. An infrared spectrum (THF) of the $[Ni_9(CO)_{18}]^{2-}$ dianion ex-

[†] Deceased.

(1) (a) University of Wisconsin—Madison. (b) Istituto di Chimica Generale dell'Universita di Milano.
(2) Calabrese, J. C.; Dahl, L. F.; Chini, P.; Longoni, G.; Martinengo, S. *J. Am. Chem. Soc.* **1974**, *96*, 2614–2616.
(3) Longoni, G.; Chini, P. *J. Am. Chem. Soc.* **1976**, *98*, 7225–7231.
(4) Lower, L. D. Ph.D. Thesis, University of Wisconsin—Madison, 1979.
(5) Calabrese, J. C.; Dahl, L. F.; Cavalieri, A.; Chini, P.; Longoni, G.; Martinengo, S. *J. Am. Chem. Soc.* **1974**, *96*, 2616–2618.
(6) Longoni, G.; Chini, P.; Cavalieri, A. *Inorg. Chem.* **1976**, *15*, 3025–3029.
(7) Longoni, G.; Chini, P. *Inorg. Chem.* **1976**, *15*, 3029–3031.

0276-7333/86/2305-1764$01.50/0

hibited strong carbonyl bands at 2005 and 1825 cm^{-1}. Salts of 1 are air-sensitive both in solution and in the solid state. Its rapid reaction with carbon monoxide to give the $[Ni_5(CO)_{12}]^{2-}$ dianion[6,8] and $Ni(CO)_4$ is in contrast to the stability of the $[Pt_9(CO)_{18}]^{2-}$ dianion toward carbon monoxide. The relatively low stability of 1 is also evidenced by its reaction with halide ions to give $[Ni_6(CO)_{12}]^{2-}$ plus decomposition products.

An X-ray diffraction examination of the $[AsPh_4]^+$ salt of 1 by Lower et al.[4,9] in 1975 established that this cluster was formed from the fusion of three parallel $Ni_3(CO)_3(\mu\text{-}CO)_3$ subunits; however, the stacking arrangement exhibited an unusual conformation which did not correspond either to a face-sharing bi(trigonal- antiprismatic) polyhedron or to a face-sharing bi(trigonal-prismatic) polyhedron observed for the $[Pt_9(CO)_{18}]^{2-}$ dianion. Unfortunately, the true conformation of 1 was obscured by a centrosymmetric crystal disorder in which the dianion was randomly distributed between two orientations related by an average center of symmetry; this crystal disorder appeared to superimpose the two outer $Ni_3(CO)_3(\mu\text{-}CO)_3$ layers to give whole-weighted atoms as well as to produce six half-weighted nickel atoms in a "Star-of-David" arrangement[10-13] for the central triangular nickel layer.

In 1981 Hall and Ruff[14] reported the preparation of $[PPN]^+_2[Ni_9(CO)_{18}]^{2-}$ in 80% yield by the reaction of $Ni(CO)_4$ with $[PPN]^+[BH_4]^-$ in CH_2Cl_2. They also obtained the $[PPN]^+$ salt of 1 in 50% yield by the reaction of $[PPN]^+_2[W_2(CO)_{10}]^{2-}$ and excess $Ni(CO)_4$ in refluxing THF. In addition, they found that 1 was converted to the $[W_2Ni_3(CO)_{16}]^{2-}$ dianion[13] when it was refluxed with $W(CO)_6$ in THF.

In connection with an extensive investigation of the diverse reactivity[15-19] of the $[Ni_6(CO)_{12}]^{2-}$ dianion, its reactions with other oxidants were studied by Nagaki and Dahl. Oxidation of the $[Ni_6(CO)_{12}]^{2-}$ dianion with iron(III) chloride in MeOH produced crystalline 1 as the $[AsPh_4]^+$ salt in nearly quantitative yield; further reaction of 1 with $FeCl_3$ in methanol yielded the $[Ni_{12}(CO)_{21}H]^{3-}$ trianion.[19,20] This recent work was partly motivated by our desire to isolate nondisordered crystals of a salt of 1 in order to obtain a relatively precise configuration that would clarify the structural-bonding nature of the Ni_9 core.

Table I. Crystal Data and Data Collection Parameters for $[AsPh_4]^+_2[Ni_9(CO)_{18}]^{2-}$

A. Crystal Data

formula	$C_{66}H_{40}O_{18}As_2Ni_9$
formula weight	1799.17
Laue group	C_{2h}—$2/m$ (monoclinic)
temperature, °C	22
a, Å	20.347 (4)
b, Å	15.758 (5)
c, Å	22.820 (8)
β, deg	114.38 (2)
V, Å^3	6663.8
Z	4
d_{calcd}, g/cm^3	1.79
space group	$P2_1/n$
$F(000)$, e	3592
μ(Mo Kα), cm^{-1}	35.5

B. Data Collection Parameters

scan mode	ω scan
scan speed, deg/min	variable (4–24)
scan width, deg	1.2
background offset, deg	1.0
background/scan time ratio	0.6667
2θ limits, deg	4–55
data collected	$\pm h,+k,+l$
no. of independent data	8703
data with $F > 3\sigma(F)$	4927

Presented herein are the results of our redetermination of the crystal structure of $[AsPh_4]^+_2[Ni_9(CO)_{18}]^{2-}$ which has fulfilled this objective. A close examination of appropriate interatomic distances has established that the three stacked triangular nickel layers in 1 roughly approximate a heretofore unknown polyhedron consisting of a trigonal antiprism fused with a trigonal prism. A geometrical-bonding comparison of 1 with the $[Pt_9(CO)_{18}]^{2-}$ dianion[2,4] and the $[Rh_9(CO)_{19}]^{3-}$ trianion[21] is also given.

Experimental Section

Materials and General Procedures. All reactions were carried out in an atmosphere of N_2 with a standard Schlenk line, stainless-steel cannulae, and drybox techniques. Solvents were dried and freshly distilled under a nitrogen atmosphere from the following solvent/desiccant combinations: C_6H_{12} (CaH_2), Et_2O (K/benzophenone ketyl), THF (K/benzophenone ketyl), and acetone (B_2O_3). $[NBu_4]^+_2[Ni_6(CO)_{12}]^{2-}$ was prepared as described previously.[5,6] Infrared spectra were taken on a Beckman Model 4240 spectrophotometer.

Preparation of $[AsPh_4]^+_2[Ni_9(CO)_{18}]^{2-}$. In a typical reaction 1.0 g of $[NBu_4]^+_2[Ni_6(CO)_{12}]^{2-}$ was dissolved in 50 mL of wet MeOH. A dilute solution of the oxidant $FeCl_3$ was slowly added dropwise to a stirred solution of $[NBu_4]^+_2[Ni_6(CO)_{12}]^{2-}$. The reaction was monitored by IR spectroscopy. After all of the $[Ni_6(CO)_{12}]^{2-}$ was converted into $[NBu_4]^+_2[Ni_9(CO)_{18}]^{2-}$, $[AsPh_4]^+Cl^-$ was added to the MeOH solution. The crude product containing the desired $[AsPh_4]^+_2[Ni_9(CO)_{18}]^{2-}$ was precipitated by the addition of H_2O. The resulting precipitate was washed exhaustively with H_2O to eliminate excess chloride ions which can readily reduce the $[Ni_9(CO)_{18}]^{2-}$ dianion back to the $[Ni_6(CO)_{12}]^{2-}$ dianion. The precipitate was then washed with ether, after which the $[AsPh_4]^+$ salt of the $[Ni_9(CO)_{18}]^{2-}$ dianion (1) was isolated from the precipitate by extraction into THF to yield a clear cherry red solution. The solvent was then either removed under vacuum or slowly evaporated with a stream of nitrogen to give crystalline $[PPh_4]^+_2[Ni_9(CO)_{18}]^{2-}$ in ca. 80% yield. An IR spectrum agreed with that reported by Longoni and Chini.[7]

Crystal Data. Suitable brilliant red crystals were grown from a solvent diffusion layering of cyclohexane over a concentrated THF solution of $[AsPh_4]^+_2[Ni_9(CO)_{18}]^{2-}$. X-ray data were collected at room temperature (22 °C) with graphite-monochromatized Mo Kα radiation on a refurbished Nicolet diffractometer (upgraded

(8) Longoni, G.; Chini, P.; Lower, L. D.; Dahl, L. F. *J. Am. Chem. Soc.* **1975**, *97*, 5034–5036.
(9) Lower, L.; Dahl, L. F.; Longoni, G.; Chini, P. *Abstracts of Papers*, 170th National Meeting of the American Chemical Society, Chicago, IL; American Chemical Society: Washington, DC, 1975; INORG 68.
(10) Other triangular metal clusters possessing a similar "Star-of-David" crystal disorder in which the metal triangle is randomly distributed between two centrosymmetrically related orientations include $Fe_3(CO)_{12}$,[11] the $[Fe_3(CO)_{11}]^{2-}$ dianion as the $[AsPh_4]^+$ salt,[12] the $[M_2Ni_3(CO)_{16}]^{2-}$ dianions (M = Mo, W) as the $[PPN]^+$ salts,[13] and the $[Ni_5(CO)_{12}]^{2-}$ dianion as the $[PPN]^+$ salt.[8]
(11) Wei, C. H.; Dahl, L. F. *J. Am. Chem. Soc.* **1969**, *91*, 1351–1355.
(12) Lo, F. Y.; Longoni, G.; Chini, P.; Lower, L. D.; Dahl, L. F. *J. Am. Chem. Soc.* **1980**, *102*, 7691–7701.
(13) Ruff, J. K.; White, R. P.; Dahl, L. F. *J. Am. Chem. Soc.* **1971**, *92*, 2159–2176.
(14) Hall, T. L.; Ruff, J. K. *Inorg. Chem.* **1981**, *20*, 4444–4446.
(15) Lower, L. D.; Dahl, L. F. *J. Am. Chem. Soc.* **1976**, *98*, 5046–5047.
(16) Montag, R. A. Ph.D. Thesis, University of Wisconsin—Madison, 1982.
(17) $[Ni_{12-x}(AsR)_x(CO)_{24-3x}]^{2-}$ (x = 2, 3): Rieck, D. F.; Montag, R. A.; McKechnie, T. S.; Dahl, L. F. *J. Am. Chem. Soc.* **1986**, *108*, 1330–1331.
(18) $[Rh_5Ni_6(CO)_{21}H_x]^{3-}$: Nagaki, D. A.; Badding, J. V.; Stacy, A. M.; Dahl, L. F. *J. Am. Chem. Soc.* **1986**, *108*, 3825–3827.
(19) Nagaki, D. A.; Dahl, L. F., manuscript in preparation.
(20) (a) $[Ni_{12}(CO)_{21}H_{4-n}]^{n-}$ (n = 2, 3): Broach, R. W.; Dahl, L. F.; Longoni, G.; Chini, P.; Schultz, A. J.; Williams, J. M. *Adv. Chem. Ser.* **1978**, *No. 167*, 93–110. (b) $[Ni_{12}(CO)_{21}]^{4-}$. Chini, P.; Longoni, G.; Manassero, M.; Sansoni, M. *Abstracts of the Eigth Meeting of the Italian Association of Crystallography*; Ferrara, 1977; Communication 34. (c) $[Ni_{12}(CO)_{21}H_{4-n}]^{n-}$ (n = 2–4): Ceriotti, A.; Chini, P.; Pergola, R. D.; Longoni, G. *Inorg. Chem.* **1983**, *22*, 1595–1598.
(21) Martinengo, S., Fumagalli, A.; Bonfichi, R.; Ciani, G.; Sironi, A. *J. Chem. Soc., Chem. Commun.* **1982**, 825–826.

from a P$\bar{1}$ to a P3F model) from a plate-like crystal (dimensions 0.5 × 0.6 × 0.2 mm) which was mounted under argon inside a Lindemann glass capillary. The dimensions and associated esd's for the chosen monoclinic unit cell were obtained from least-squares analysis of the setting angles for 25 well-centered reflections with $10° \leq 2\theta \leq 25°$; the symmetry of this unit cell was verified from axial photographs. An application of the cell-reduction program, TRACER,[22] ruled out any possibility of higher crystal symmetry. Crystal data and data-collection parameters are given in Table I. The intensities of three selected standard reflections (monitored after every 47 data) did not vary by more that 4% during data collection. A pseudoellipsoidal empirical absorption correction performed with 351 ψ scan data reduced the $R_1(F)$ merge value from 8.3% to 2.0% for the 351 data. The monoclinic space group $P2_1/n$ was uniquely determined from the systematic absences of $\{h0l\}$ for $h + l$ odd and $\{0k0\}$ for k odd.[23]

Structural Determination and Refinement. The structural determination involved the location of one formula species. Initial coordinates for the two independent As atoms and four of the nine independent Ni atoms were obtained by direct methods. The other non-hydrogen atoms were located from successive Fourier syntheses cycled with cascading block-matrix least-squares refinement of the positional and isotropic thermal parameters. Idealized trigonal positions for the phenyl hydrogen atoms were calculated by use of a C–H bond length of 0.96 Å. Least-squares refinement with anisotropic thermal parameters and individual positional parameters for all non-hydrogen atoms and with fixed positional and thermal parameters for all hydrogen atoms converged at $R_1(F) = 8.49\%$ and $R_2(F) = 7.01\%$. The goodness-of-fit value was 1.53, and the largest shift-to-esd ratio in the last cycle was 0.157. A separate least-squares refinement with each of the eight phenyl rings for the two independent $[AsPh_4]^+$ counterions constrained as an idealized hexagonal ring with a C–C distance of 1.39 Å gave a better data-to-parameter ratio (4927/760 = 6.5 vs. 4927/856 = 5.8) but higher values of $R_1(F)$ (8.66%) and $R_2(F)$ (7.37%); this latter model yielded essentially equivalent errors in the positional and thermal parameters. Of importance is that a comparative analysis of the two models showed the corresponding positional parameters for the atoms in the $[Ni_9(CO)_{18}]^{2-}$ dianion to be within 1 esd. Therefore, only the structural parameters based on the refinement with nonconstrained atomic positional parameters for the monocations are presented here. Final electron density difference maps based on both refinements showed no unusual features.

Atomic positional and mean isotropic thermal parameters are presented in Table II, and selected interatomic distances for the dianion are given in Table III. Anisotropic thermal parameters for all non-hydrogen atoms, interatomic distances for the monocations, and bond angles for the dianion are available as supplementary material. Observed and calculated structure factor amplitudes are also available as supplementary material. Neutral atomic scattering factors with anomalous dispersion corrections for all non-hydrogen atoms were taken from ref 24. The computer programs were those of SHELXTL (1984 version), and all computations were performed on an Eclipse S/4 system.

Results and Discussion

General Description of the Crystal Structure of $[AsPh_4]^+_2[Ni_9(CO)_{18}]^{2-}$. The solid-state structure consists of eight discrete $[AsPh_4]^+$ monocations and four $[Ni_9(CO)_{18}]^{2-}$ dianions situated in general fourfold equivalent positions in the unit cell. There are no unusually short contact distances between the cations and dianions with the shortest C(Ph)···OC distance being 4.3 Å. The configurations of the two independent $[AsPh_4]^+$ monocations

Table II. Atomic Coordinates (×10⁴) and Isotropic Thermal Parameters (Å² × 10³) for the $[Ni_9(CO)_{18}]^{2-}$ Dianion

	x	y	z	U
Ni(1)	5340 (1)	3198 (1)	2608 (1)	56 (1)*
Ni(2)	4923 (1)	3764 (1)	1539 (1)	63 (1)*
Ni(3)	4080 (1)	3466 (1)	2002 (1)	60 (1)*
Ni(4)	4733 (1)	4660 (1)	2956 (1)	58 (1)*
Ni(5)	5707 (1)	4905 (1)	2659 (1)	68 (1)*
Ni(6)	4512 (1)	5242 (1)	1934 (1)	73 (1)*
Ni(7)	5269 (1)	6187 (1)	3522 (1)	96 (1)*
Ni(8)	5895 (1)	6601 (1)	2878 (1)	86 (1)*
Ni(9)	4616 (1)	6783 (2)	2486 (1)	96 (1)*
C(1)	6030 (8)	2667 (11)	3275 (8)	69 (9)*
O(1)	6441 (6)	2294 (8)	3661 (6)	110 (8)*
C(12)	5809 (7)	3256 (8)	2032 (7)	63 (8)*
O(12)	6355 (5)	3042 (6)	2011 (5)	88 (6)*
C(2)	5032 (10)	3950 (11)	831 (9)	90 (11)*
O(2)	5109 (8)	4072 (8)	369 (6)	120 (9)*
C(23)	3913 (8)	3530 (11)	1139 (8)	77 (9)*
O(23)	3470 (6)	3424 (10)	635 (6)	123 (8)*
C(3)	3244 (8)	3385 (11)	1983 (9)	87 (9)*
O(3)	2674 (7)	3299 (8)	1991 (7)	128 (9)*
C(13)	4568 (7)	2676 (9)	2657 (7)	67 (8)*
O(13)	4394 (5)	2117 (7)	2918 (5)	99 (6)*
C(4)	4379 (8)	4235 (8)	3491 (6)	65 (8)*
O(4)	4166 (6)	3967 (8)	3823 (5)	114 (8)*
C(45)	5754 (11)	4492 (11)	3438 (8)	101 (11)*
O(45)	6148 (6)	4325 (7)	3970 (5)	92 (6)*
C(5)	6609 (9)	4879 (13)	2868 (8)	100 (9)*
O(5)	7232 (7)	4737 (8)	3019 (6)	119 (8)*
C(56)	5372 (8)	5409 (9)	1810 (7)	75 (8)*
O(56)	5601 (6)	5670 (6)	1454 (5)	90 (6)*
C(6)	3845 (10)	5547 (10)	1234 (12)	151 (14)*
O(6)	3482 (8)	5761 (9)	687 (7)	151 (10)*
C(46)	3891 (10)	5084 (11)	2328 (9)	84 (10)*
O(46)	3277 (7)	5254 (7)	2259 (6)	97 (7)*
C(7)	5249 (11)	5949 (14)	4267 (10)	110 (13)*
O(7)	5281 (11)	5788 (12)	4756 (7)	186 (13)*
C(78)	6285 (8)	6421 (10)	3791 (8)	94 (9)*
O(78)	6814 (6)	6449 (9)	4233 (6)	144 (8)*
C(8)	6677 (9)	6767 (12)	2759 (8)	89 (10)*
O(8)	7169 (7)	6873 (9)	2648 (7)	124 (9)*
C(89)	5261 (8)	7286 (9)	2209 (7)	83 (9)*
O(89)	5269 (7)	7775 (7)	1820 (7)	138 (9)*
C(9)	3802 (9)	7298 (14)	1898 (10)	96 (12)*
O(9)	3333 (8)	7632 (13)	1602 (8)	172 (12)*
C(79)	4357 (10)	6690 (11)	3203 (9)	96 (11)*
O(79)	3883 (7)	6934 (8)	3323 (7)	128 (9)*

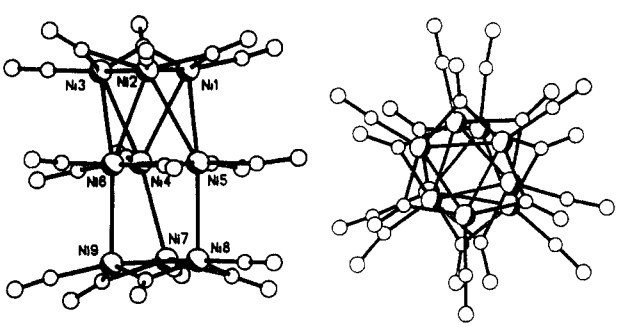

Figure 1. Two views of the pseudo C_3 geometry of the $[Ni_9(CO)_{18}]^{2-}$ dianion (1) showing the parallel stacking pattern of the three $Ni_3(CO)_3(\mu\text{-}CO)_3$ layers and resulting dispositions of the carbonyl ligands about the Ni_9 core. The left-side view reveals a considerable bending of the carbonyl ligands in both outer layers away from the inner layer. A small but detectable bending of the inner-layer carbonyl ligands is observed, involving out-of-plane displacements of the three terminal carbonyl groups toward the top layer and of the three bridging carbonyl groups toward the bottom layer. The right-side view (normal to the central nickel triangle) reveals (1) that the top $Ni_3(CO)_3(\mu\text{-}CO)_3$ layer is oriented in an approximate antiprismatic conformation with respect to the middle $Ni_3(CO)_3(\mu\text{-}CO)_3$ layer such that each terminal carbonyl carbon atom in either of these two layers is situated almost over a bridging carbonyl oxygen atom in the other layer and (2) that the bottom $Ni_3(CO)_3(\mu\text{-}CO)_3$ layer is oriented in a nearly eclipsed conformation with respect to the middle $Ni_3(CO)_3(\mu\text{-}CO)_3$ layer.

(22) Lawton, S. L.; Jacobson, R. A TRACER—The Reduced Cell and Its Crystallographic Applications; Ames Laboratories, Iowa State University: Ames, IA, 1965; IS-1141.

(23) The nonstandard space group $P2_1/n$ can be converted to the standard space group $P2_1/c$ (C^5_{2h}—no. 14) by an axial transformation to a different unit cell. Coordinates of the general fourfold equivalent positions for $P2_1/n$ are as follows: x, y, z; $-x, -y, -z$; $^1/_2 + x, ^1/_2 - y, ^1/_2 + z$; $^1/_2 - x, ^1/_2 + y, ^1/_2 - z$.

(24) *International Tables for X-ray Crystallography*; 2nd ed.; Kynoch Press: Birmingham, England, 1965; Vol. IV, pp 149, 155–157.

Table III. Interatomic Distances (Å) for the $[Ni_9(CO)_{18}]^{2-}$ Dianion (1)

A. Intertriangular Ni–Ni Distances[a]

Ni(1)–Ni(5)	2.782 (3)	Ni(1)–Ni(4)	2.876 (3)
Ni(2)–Ni(6)	2.749 (3)	Ni(2)–Ni(5)	2.989 (3)
Ni(3)–Ni(4)	2.766 (3)	Ni(3)–Ni(6)	2.957 (3)
	2.766 (av)		2.941 (av)
Ni(4)–Ni(7)	2.736 (3)		
Ni(5)–Ni(8)	2.717 (3)		
Ni(6)–Ni(9)	2.704 (3)		
	2.719 (av)		

B. Intratriangular Ni–Ni Distances[a]

Ni(1)–Ni(2)	2.400 (3)	Ni(4)–Ni(5)	2.376 (4)
Ni(1)–Ni(3)	2.395 (3)	Ni(4)–Ni(6)	2.369 (4)
Ni(2)–Ni(3)	2.405 (3)	Ni(5)–Ni(6)	2.368 (3)
	2.400 (av)		2.371 (av)
Ni(7)–Ni(8)	2.367 (4)		
Ni(7)–Ni(9)	2.374 (3)		
Ni(8)–Ni(9)	2.395 (4)		
	2.389 (av)		

C. Ni–CO(terminal) Distances

Ni(1)–C(1)	1.79 (1)
Ni(2)–C(2)	1.75 (2)
Ni(3)–C(3)	1.69 (2)
Ni(4)–C(4)	1.79 (2)
Ni(5)–C(5)	1.70 (2)
Ni(6)–C(6)	1.68 (2)
Ni(7)–C(7)	1.76 (3)
Ni(8)–C(8)	1.74 (2)
Ni(9)–C(9)	1.84 (2)
	1.75 (av)

D. Ni–CO(bridging) Distances

Ni(1)–C(12)	1.92 (2)
Ni(1)–C(13)	1.82 (2)
Ni(2)–C(23)	1.91 (2)
Ni(2)–C(12)	1.87 (1)
Ni(3)–C(13)	1.88 (1)
Ni(3)–C(23)	1.86 (2)
Ni(4)–C(45)	1.93 (2)
Ni(4)–C(46)	1.85 (2)
Ni(5)–C(56)	1.94 (2)
Ni(5)–C(45)	1.86 (2)
Ni(6)–C(46)	1.85 (2)
Ni(6)–C(56)	1.90 (2)
Ni(7)–C(78)	1.93 (2)
Ni(7)–C(79)	1.87 (2)
Ni(8)–C(89)	1.88 (1)
Ni(8)–C(78)	1.92 (2)
Ni(9)–C(79)	1.92 (2)
Ni(9)–C(89)	1.86 (2)
	1.89 (av)

E. C–O(terminal) and C–O(bridging) Distances

Terminal	
C(1)–O(1)	1.10 (2)
C(2)–O(2)	1.14 (3)
C(3)–O(3)	1.18 (2)
C(4)–O(4)	1.10 (2)
C(5)–O(5)	1.19 (2)
C(6)–O(6)	1.21 (3)
C(7)–O(7)	1.12 (3)
C(8)–O(8)	1.14 (3)
C(9)–O(9)	1.06 (2)
	1.14 (av)
Bridging	
C(12)–O(12)	1.18 (2)
C(23)–O(23)	1.14 (2)
C(13)–O(13)	1.20 (2)
C(45)–O(45)	1.18 (2)
C(56)–O(56)	1.17 (2)
C(46)–O(46)	1.22 (3)
C(78)–O(78)	1.13 (2)
C(89)–O(89)	1.18 (2)
C(79)–O(79)	1.17 (3)
	1.17 (av)

[a] Averaged under assumed C_3 symmetry.

are expectedly similar and exhibit no unusual features from those found in the crystal structures of other tetraphenylarsonium salts.

Structural Features of the $[Ni_9(CO)_{18}]^{2-}$ Dianion. (a) Overall Configuration. The architecture (Figure 1) of 1 consists of a stacking of three planar $[Ni_3(CO)_3(\mu\text{-}CO)_3]$ subunits whose orientations approximately conform to a

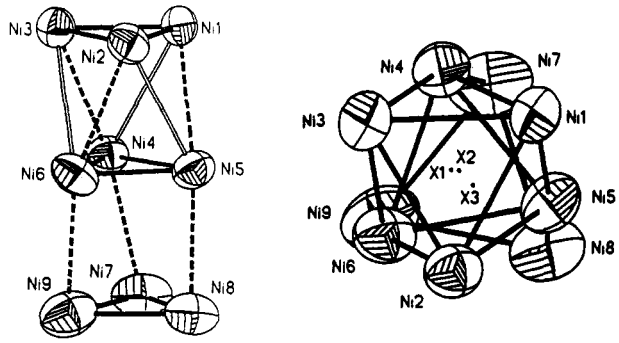

Figure 2. Two views of the (triangular metal)-stacked conformation of the Ni_9 core which may be envisioned as resulting from a trigonal prismatic capping of a triangular face of a trigonal antiprismatic Ni_6 fragment (formed from the top and middle Ni_3 triangles) by the bottom Ni_3 triangle. The centroid of each Ni_3 triangle in the right-side view (down the pseudo threefold axis) is designated by X*n*, where X1 is that for the top triangle (formed by Ni1, Ni2, Ni3), X2 is that for the middle triangle (formed by Ni4, Ni5, Ni6), and X3 is that for the bottom triangle (formed by Ni7, Ni8, Ni9). The observed twisting deformation (by 9° about the pseudo threefold axis) of the Ni_6 fragment defined by the top and middle Ni_3 triangles from a regular trigonal-antiprismatic conformation gives rise to three shorter, bonding intertriangular Ni–Ni distances (denoted by dashed–solid lines) of mean 2.77 Å and three longer, weakly bonding intertriangular Ni–Ni distances (denoted by hollow lines) of mean 2.94 Å. The angular distortion (by 21° about the pseudo threefold axis) of the Ni_6 fragment defined by the middle and bottom Ni_3 triangles from a regular trigonal-prismatic conformation produces three bonding intertriangular Ni–Ni distances (denoted by dashed-solid lines) of mean 2.72 Å. The nine similar intratriangular Ni–Ni distances (denoted by full-solid lines) for the three Ni_3 triangles average 2.39 Å.

C_3 geometry with the pseudo threefold axis perpendicular to the planes of the three Ni_3 subunits. A close examination of the observed three-layer pattern and the intertriangular and intratriangular Ni–Ni distances (vide infra) indicates that the conformation of 1 is best described as arising from the fusion of a trigonal prism and a trigonal antiprism on a common triangular face. Figure 2, which shows two views of the Ni_9 core of 1, reveals considerable rotational and translational distortions from an idealized C_{3v} geometry to the observed pseudo C_3 geometry.

(b) Triangular Nickel Stacking of the Ni_9 Core. Of prime interest is the nature of stacking of the three individual $Ni_3(CO)_3(\mu\text{-}CO)_3$ subunits, designated as layers A, B, and C. The essentially parallel stacking of these layers is evidenced by the interplanar angles of 1.3° between layers A and B, 1.7° between layers B and C, and 2.1° between layers A and C.

Figure 2 reveals that the three layers possess an irregular arrangement which does not conform either to a regular-eclipsed conformation corresponding to a face-sharing bi(trigonal-prismatic) polyhedron or to a regular-staggered conformation corresponding to a face-sharing bi(trigonal-antiprismatic) polyhedron. The top Ni_3 triangle (layer A) is staggered by ca. 51° relative to the middle Ni_3 triangle (layer B), which results in layers A and B forming a trigonal antiprism of six nickel atoms that is deformed from a regular trigonal antiprismatic geometry by a rotational twist of −9° about the pseudo threefold axis. The bottom Ni_3 triangle (layer C) is staggered by ca. 21° relative to the middle Ni_3 triangle (layer B), which results in layers B and C forming a helically distorted trigonal prism of six nickel atoms. This angular disposition results in the two outer triangles, A and C, being staggered by ca. 49° relative to one another (vs. 60° for a centrosymmetric conformation).

Figure 2 also indicates a relatively small lateral slip between the Ni_3 triangles A and B compared to that be-

tween the Ni_3 triangles B and C. In accordance with this difference in translational distortion, the centroids for the external triangles A and C, when projected onto the interior triangle B, are displaced by ca. 0.05 and 0.20 Å, respectively, from the centroid of triangle B.

The perpendicular interplanar distance between the triangular Ni_3 layers A and B is 2.49 Å, while that between the triangular Ni_3 layers B and C is 2.66 Å. The considerably shorter interplanar AB distance, which signifies that the trigonal antiprismatic $[Ni_3(CO)_3(\mu\text{-}CO)_3]_2$ fragment AB is compressed along the pseudo threefold axis relative to the trigonal-prismatic $[Ni_3(CO)_3(\mu\text{-}CO)_3]_2$ fragment BC, is consistent with the interplanar distances between adjacent Ni_3 layers found in the $[Ni_6(CO)_{12}]^{2-}$ dianion (2.49 Å)[5] and in the $[Ni_{12}(CO)_{21}H_n]^{n-4}$ anions (n = 0–2)[19,20] (e.g., 2.56 and 2.53 Å the $[NMe_4]^+$ salt of the monohydrido trianion (n = 1)[19]).

A further examination of Figure 2 shows that the atomic thermal ellipsoids for the three nickel atoms in layer C are significantly larger than those for the nickel atoms in layers A and B. This difference is attributed to the trigonal-antiprismatic nickel atoms in triangles A and B being more tightly locked into their equilibrium positions (with resulting smaller thermal motion) than are the capping trigonal-prismatic nickel atoms in triangle C.

(c) Intertriangular Nickel–Nickel Distances. A striking structural consequence of the pseudo C_3 geometry observed for the Ni_9 core is the effect on the Ni–Ni distances between the nickel triangles A and B, which form a primarily twisted trigonal antiprism, and those between the nickel triangles B and C, which form a translationally and angularly distorted trigonal prism.

The Ni–Ni distances between layers A and B fall into two distinct groups. The first group consists of three relatively normal Ni–Ni distances which vary from 2.749 (3) to 2.782 (3) Å; the mean of 2.77 Å is identical with that of 2.77 Å for the six equivalent intertriangular Ni–Ni distances in the regular trigonal-antiprismatic $[Ni_6(CO)_{12}]^{2-}$ dianion[5] and compares well with those of 2.80 and 2.83 Å for the two sets of six intertriangular Ni–Ni distances in the two trigonal-antiprismatic fragments in the $[Ni_{12}(CO)_{21}H]^{3-}$ trianion.[19] The second group of three Ni–Ni distances ranges from 2.876 (3) to 2.989 (3) Å with a mean value of 2.94 Å. These 0.17 Å longer Ni–Ni distances point to relatively weak Ni–Ni interactions. The distorted C_3 geometry which results in the metal–metal bonding between layers A and B being mainly due to three Ni–Ni interactions instead of six interlayer Ni–Ni interactions (as found in the regular antiprismatic $[Ni_6(CO)_{12}]^{2-}$ dianion) is attributed to interlayer carbonyl repulsions (vide infra).

The three bonding intertriangular Ni–Ni distances between layers B and C vary from 2.704 (3) to 2.736 (3) Å. The mean of 2.72 Å is comparable to that of 2.65 Å for the intertriangular Ni–Ni distances in the pentacapped trigonal-prismatic $Ni_6(\mu_3\text{-}C)(\mu_3\text{-}P)(\mu_4\text{-}P)_3$ core of $Ni_6(CO)_6(\mu_3\text{-}CO)(\mu_3\text{-}P\text{-}t\text{-}Bu)(\mu_4\text{-}P\text{-}t\text{-}Bu)_3$.[16]

(d) Intratriangular Nickel–Nickel Distances. The three Ni–Ni bond distances in each of the outer two triangular nickel layers (of range 2.395 (3)–2.405 (3) Å and mean 2.40 Å in layer A and range 2.374 (3)–2.397 (4) Å and mean 2.39 Å in layer C) are close to those (of range 2.368 (3)–2.376 (4) Å and mean 2.37 Å) in the central triangular nickel layer B. The average value of 2.39 Å for these nine intratriangular carbonyl-bridged Ni–Ni bonds is in good agreement with those of the intratriangular carbonyl-bridged Ni–Ni bonds in the corresponding $Ni_3(CO)_3(\mu\text{-}CO)_3$ fragments contained in the $[Ni_6(CO)_{12}]^{2-}$ dianion (2.38 Å)[5] and in the $[Ni_{12}(CO)_{21}H]^{3-}$ trianion (2.42 Å).[19] The slightly shorter intratriangular Ni–Ni distances found in the central $Ni_3(CO)_3(\mu\text{-}CO)_3$ part of the $[Ni_5(CO)_{12}]^{2-}$ dianion (2.36 Å)[8] and of the isostructural $[M_2Ni_3(CO)_{16}]^{2-}$ dianions (2.34 Å for M denoting both Mo and W)[13] may reflect a much greater uncertainty due to a crystallographically imposed centrosymmetric disorder in each of these dianions.[10]

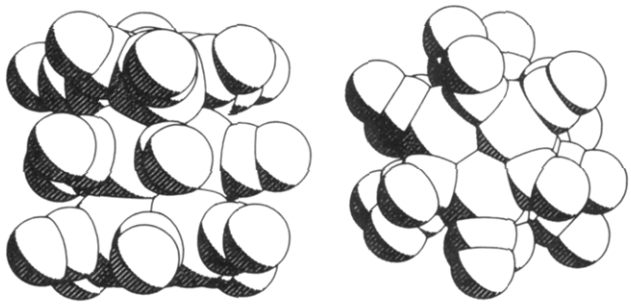

Figure 3. Two views (analogous to those in Figure 1) of space-filling atomic models which more realistically depict the steric dispositions of the terminal and bridging carbonyl ligands in the three stacked $Ni_3(CO)_3(\mu\text{-}CO)_3$ layers.

The above distances for the intratriangular carbonyl-bridged Ni–Ni bonds are also similar to the Ni–Ni distance of 2.390 (1) Å in the planar $Ni_2(CO)_2$ core of $Ni_2(\eta^5\text{-}C_5H_4Me)_2(\mu_2\text{-}CO)_2$[25] and to those of 2.363 (1) and 2.351 (1) Å for the differently bent nonplanar $Ni_2(CO)_2$ cores in the two crystallographically independent molecules of $[Ni(\eta^5\text{-}C_5H_5)(\mu\text{-}CO)]_2$.[25,26]

(e) The Carbonyl Ligands: Their Disposition and Resulting Implications. The average Ni–CO(terminal) and Ni–CO(bridging) bond lengths of 1.75 and 1.89 Å, respectively, in **1** are in excellent agreement with the corresponding values of 1.75 and 1.90 Å in the $[Ni_6(CO)_{12}]^{2-}$ dianion.

Strong repulsions between the carbonyl ligands of the central and outer triangular nickel subunits in **1** (Figure 3) are evidenced from results of least-squares plane calculations which show that the carbonyl ligands are significantly displaced from all three Ni_3 planes. In layer A the terminal and bridging carbonyl carbon atoms are displaced above the Ni_3 plane by 0.22 and 0.56 Å, respectively. In layer C the terminal and bridging carbonyl carbon atoms are analogously displaced below the Ni_3 plane (away from layer B) by 0.22 and 0.49 Å, respectively. Much smaller but still significant bending of the carbonyl ligands is also found in layer B, where the three terminal and three bridging carbonyl carbon atoms display average displacements of ca. 0.1 Å in opposite directions; the terminal carbonyl carbon atoms have an average out-of-plane displacement of 0.08 Å toward layer A, whereas the bridging carbonyl carbon atoms have an average out-of-plane displacement of 0.09 Å toward layer C. The shortest OC···CO contacts are 3.1 Å between layers A and B and 3.2 Å between layers B and C.

Similar out-of-plane distortions found in the $[Ni_6(CO)_{12}]^{2-}$ dianion were also ascribed to interplanar carbonyl repulsions.[5] This tilting of the carbonyl ligands in the outer two layers away from the central triangle is much less pronounced in the $[Pt_9(CO)_{18}]^{2-}$ dianion due to the considerably larger distance of 3.0 Å between adjacent $Pt_3(CO)_3(\mu\text{-}CO)_3$ subunits.[2,4] Hoffmann and co-workers[40] recently pointed out that in addition to minimizing inter-

(25) Byers, L. R.; Dahl, L. F. *Inorg. Chem.* **1980**, *19*, 680–692.
(26) Madach, T.; Fischer, K.; Vahrenkamp, H. *Chem. Ber.* **1980**, *113*, 3235–3244.

planar ligand repulsions, the out-of-plane deformations of the carbonyl ligands can give rise to stronger M–M bonding between adjacent stacked $M_3(CO)_3(\mu\text{-}CO)_3$ subunits due primarily to a change in metal hybridization.

Geometrical-Bonding Relationship of the Ni_9 Core in $[Ni_9(CO)_{18}]^{2-}$ (1) with the Pt_9 Core in $[Pt_9(CO)_{18}]^{2-}$ (2) and the Rh_9 Core in $[Rh_9(CO)_{19}]^{3-}$ (3) and Resulting Implications. (a) Comparison of (Triangular Metal)-Stacked Geometries. The Ni_9 core of 1 provides the first example of a face-sharing (trigonal-antiprismatic)–(trigonal-prismatic) polyhedron. This particular conformer of three (triangular metal)-stacked layers may be considered as a geometrical hybrid of a face-sharing bi(trigonal-antiprismatic) D_{3h} polyhedron and a face-sharing bi(trigonal-prismatic) D_{3h} polyhedron.

The face-sharing bi(trigonal-antiprismatic) D_{3h} polyhedron (alternatively designated as a bioctahedral polyhedron[27]) is exemplified by the Rh_9 core in the $[Rh_9(CO)_{19}]^{3-}$ trianion (3).[21] Of interest is that this face-sharing bioctahedral Rh_9 core is a geometrical extension of the octahedral Rh_6 core in $Rh_6(CO)_{16}$.[28] Moreover, the Rh_9 core can also be extended by a staggered face-capping along the pseudo threefold axis with a triangular Rh_3 fragment to give a face-sharing trioctahedral Rh_{12} core which was found in the recently reported $Rh_{12}H_2(CO)_{25}$.[29] Other species containing a stack of three staggered metal triangles formed by two condensed trigonal antiprisms (or octahedra) sharing a common triangular face include the $[Ni_9S_9(PEt_3)_6]^{2+}$ dication[30] and the Mo_9Se_{11} unit in $In_{\sim 3}Mo_{15}Se_{19}$;[31] both of these bioctahedral or bi(trigonal-antiprismatic) metal cores are held together by face-capping chalcogenide atoms.

The face-sharing bi(trigonal-prismatic) D_{3h} polyhedron, which represents the other known regular stacking pattern of three metal triangles, is illustrated by the Pt_9 core in the $[Pt_9(CO)_{18}]^{2-}$ dianion (2). This conformer is one member of the $[Pt_3(CO)_6]_n^{2-}$ series (n = 2–5) of oligomers whose idealized D_{3h} geometries involve an eclipsed superposition of $Pt_3(CO)_3(\mu\text{-}CO)_3$ building blocks.[2-4]

These three types of nonametal cores represent the three regular-stacked conformers which can be constructed from three superimposed equilateral metal triangles with different rotational sequences along the principal threefold axis. In all cases, small relative rotations and translational displacements from idealized geometries are observed.

The conformational transformation from a trigonal-antiprismatic metal arrangement in the $[Ni_6(CO)_{12}]^{2-}$ dianion to a trigonal-prismatic one in the corresponding $[Pt_6(CO)_{12}]^{2-}$ dianion was attributed to both electronic and steric effects.[5] In addition to the inherently stronger Pt–Pt bonding stabilizing a trigonal prismatic conformation with only three intertriangular Pt–Pt distances, it was presumed that the considerably smaller interlayer separation due to shorter intertriangular Ni–Ni distances of 2.77 Å vs. corresponding Pt–Pt distances of 3.04 Å necessitated a staggered conformation for the $[Ni_6(CO)_{12}]^{2-}$ dianion in order to minimize carbonyl repulsive forces.

X-ray photoemission spectra of the $[Pt_3(CO)_6]_n^{2-}$ dianions were found by Apai et al.[33] to display remarkably similar 5d Pt-derived bands. Observed shifts in the binding energies of the carbonyl orbitals (5σ and 1π) to higher values with an increase in cluster size were interpreted as due to the decreasing effect of the anion charge in the larger clusters and to the bonding character of the carbonyl orbitals.[33] On this basis it was concluded that negligible interactions exist between the $Pt_3(CO)_3(\mu\text{-}CO)_3$ layers.

This indication that interlayer interactions in the $[Pt_3(CO)_6]_n^{2-}$ dianions are small is in accordance with an analysis by Heaton and co-workers[34] of their ^{195}Pt NMR solution spectra. They observed that spectra both at 25° and −85° for the $[Pt_9(CO)_{18}]^{2-}$ dianion (2) are consistent with rapid rotation of the outer Pt_3 triangles with respect to the middle Pt_3 triangle about the pseudo threefold axis.[34a] Furthermore, mixed solutions of the $[Pt_9(CO)_{18}]^{2-}$ and $[Pt_{12}(CO)_{24}]^{2-}$ dianions displayed at 25° only a very broad ^{195}Pt signal which was attributed to an interexchange of Pt_3 triangles between the two clusters. Heaton and co-workers[34b] subsequently determined that intertriangular exchange between different clusters (or self-exchange) occurs when clusters contain inner Pt_3 triangles (for which carbonyl distortions are limited). The increased lability of the clusters (with $n \geq 3$) with increased size was ascribed to a relative destabilization due to greater interlayer carbonyl repulsions. ^{13}C NMR spectra (−100 to +60 °C) of the $[Pt_3(CO)_6]_n^{2-}$ dianions (n = 2–4) showed no terminal/bridge carbonyl intraexchange in contrast to a room-temperature spectrum of the $[Ni_6(CO)_{12}]^{2-}$ dianion showing terminal/bridge carbonyl exchange. Heaton and co-workers[34a] pointed out that the $[Pt_9(CO)_{18}]^{2-}$dianion is the first example of a cluster undergoing an internal metal polyhedral conformational change and that this phenomenon is presumably related to a small difference in energies between trigonal-prismatic and trigonal-antiprismatic structures.

The hybrid conformation of 1 may be considered as a static representation of an intermediate (or transition state) through which 2 must traverse in accounting for its fluxional behavior in solution via independent intratriangular rotation about the pseudo threefold axis. The fact that the $[Pt_3(CO)_6]_n^{2-}$ dianions ($n \geq 3$) also undergo intertriangular exchange in solution supports the premise that the $[Ni_9(CO)_{18}]^{2-}$ dianion is derived from the trigonal prismatic addition of a third $Ni_3(CO)_6$ subunit to the trigonal-antiprismatic $[Ni_6(CO)_{12}]^{2-}$ dianion.

(b) Bonding Analysis via Electron-Counting Schemes. The three different idealized conformers lead to a different number of *intertriangular* metal–metal bonds—viz., *six* for the bi(trigonal-prismatic) D_{3h} Pt_9 core in **2**, *nine* for the (trigonal-antiprismatic)–(trigonal-prismatic) C_{3v} Ni_9 core in **1**, and *twelve* for the bi(trigonal-antiprismatic) D_{3h} Rh_9 in **3**. Hence, it is presumed that the particular conformation adopted by the (triangular metal)-stacked core of a metal carbonyl cluster depends upon electronic effects (in the absence of unusual steric

(27) Our current preference that the Ni_6 core of the D_{3d} $[Ni_6(CO)_{12}]^{2-}$ dianion[5] is more precisely formulated as a trigonal-antiprismatic polyhedron rather than an octahedral-like polyhedron is based upon the large difference of 0.4 Å between the six intratriangular and six intertriangular Ni–Ni distances which for a regular octahedron would have equivalent values. Similar Ni–Ni bond-length differences in the $[Ni_9(CO)_{18}]^{2-}$ dianion (1) likewise suggest that it is better described as a face-fused (trigonal-antiprismatic)–(trigonal-prismatic) polyhedron instead of a face-fused octahedral–(trigonal-prismatic) polyhedron.

(28) Corey, E.; Dahl, L. F.; Beck, W. *J. Am. Chem. Soc.* **1963**, *85*, 1202–1203.

(29) Ciani, G.; Sironi, A.; Martinengo, S. *J. Chem. Soc., Chem. Commun.* **1985**, 1757–1759.

(30) (a) Ghilardi, C. A.; Midollini, S.; Sacconi, L. *J. Chem. Soc., Chem. Commun.* **1981**, 47–48. (b) Cecconi, F.; Ghilardi, C. A.; Midollini, S. *Inorg. Chem.* **1983**, *22*, 3802–3808.

(31) Grüttner, A.; Yvon, K.; Chevrel, R.; Potel, M.; Sergent, M.; Seeber, B. *Acta Crystallog., Sect. B: Struct. Crystallogr. Cryst. Chem.* **1979**, *B35*, 285–292.

(32) Lauher, J. W. *J. Am. Chem. Soc.* **1978**, *100*, 5305–5315.

(33) Apai, G.; Lee, S.-T.; Mason, M. G.; Gerenser, L. J.; Gardner, S. A. *J. Am. Chem. Soc.* **1979**, *101*, 6880–6883.

(34) (a) Brown, C.; Heaton, B. T.; Chini, P.; Fumagalli, A.; Longoni, G. *J. Chem. Soc., Chem. Commun.* **1977**, 309–311. (b) Brown, C.; Heaton, B. T.; Towl, A. D. C.; Chini, P.; Fumagalli, A.; Longoni, G. *J. Organomet. Chem.* **1979**, *181*, 233–254.

interactions). In agreement with this notion, the observed number of metal cluster valence electrons[32] is 128 for both **1** and **2** and 122 for **3**. Both the polyhedral skeletal electron-pair approach[35] adopted by Mingos[36] for condensed polyhedra and the topological electron-counting model of Teo[37] predict electron counts of 128 for **1**, 132 for **2**, and 124 for **3**.[38] The agreement between the predicted and observed electron counts for the Ni_9 core in **1** suggests that the origin of its hybrid geometry is indeed electronic.[39,40]

The observed value of 122 electrons for the bioctahedral Rh_9 core in **3** is two electrons less than the predicted value.[36c,37b,38,41,42] Analogously, the observed value of 160 electrons for the face-condensed trioctahedral Rh_{12} core in $Rh_{12}H_2(CO)_{25}$[29] is also two electrons less than the predicted value.[36c,37b,38]

The fact that the observed count of 128 electrons for the Pt_9 core in **2** is 4 electrons less than the predicted count is not surprising since each of the similarly stacked $[Pt_3(CO)_6]_n^{2-}$ dianions (n = 2–5) has 4 electrons less than the expected value. The tendency of these triangular platinum carbonyl clusters to be 4–6 electrons under the required electron counts has been ascribed by others[32,36a,37b,40,43] to two or three high-energy MO's composed primarily of out-of-plane valence 6p(Pt) AO's being unoccupied.

By use of graph theory,[44] King[45,46] proposed a skeletal bonding model for the $[Pt_3(CO)_6]_n^{2-}$ clusters; in the case of the $[Pt_9(CO)_{18}]^{2-}$ dianion (**2**), his model would involve edge-localized bonding along the 15 edges of the bi(trigonal-prismatic)Pt_9 core coupled with additional Möbius-type bonding in the two outer triangular platinum layers. In an extension of the King graph model[45,46] to the Ni_9 core of **1**, we have assumed that **1** arises from an eclipsed capping of a $Ni_3(CO)_6$ fragment (with its 12 skeletal electrons involved in six edge-localized electron-pair bonds) to a triagular face of the trigonal-antiprismatic $[Ni_6(CO)_{12}]^{2-}$ dianion (with its 14 skeletal electrons involved in delocalized bonds). This model, which views the Ni_9 polyhedron in terms of delocalized skeletal bonding in the trigonal-antiprismatic fragment and edge-localized bonding in the trigonal-prismatic cap, appears to be consistent with the Mingos rules[36] for condensed polyhedra.[47-50] Although this localized-delocalized bonding description appears to be plausible for the Ni_9 core in **1**, in this case it cannot be regarded as an adequate explanation for the existence of the structure. It is apparent that a detailed MO examination of **1** is needed.[51,52]

(c) Molecular Orbital Considerations. The close correlation between the corresponding intralayer distances and bond angles within the $Ni_3(CO)_3(\mu\text{-}CO)_3$ layers of the $[M_2Ni_3(CO)_{16}]^{2-}$ (M = Mo, W), $[Ni_5(CO)_{12}]^{2-}$, and $[Ni_6(CO)_{12}]^{2-}$ dianions led to the hypothesis[5,8] that the intralayer bonding in the latter two dianions parallels that in the $[M_2Ni_3(CO)_{16}]^{2-}$ dianions.[13] A qualitative MO bonding

(35) (a) Wade, K. *J. Chem. Soc., Chem. Commun.* **1971**, 792–793. (b) Wade, K. *Electron Deficient Compounds*; Thomas Nelson and Sons, Ltd.: London, 1971. (c) Wade, K. *Chem. Br.* **1975**, *11*, 177–183. (d) Wade, K. *Adv. Inorg. Chem. Radiochem.* **1976**, *18*, 1–66. (e) Mingos, D. M. P. *Nature (London), Phys. Sci.* **1972**, *236*, 99–102. (f) Mingos, D. M. P.; Forsyth, M. I. *J. Chem. Soc., Dalton Trans.* **1977**, 610–616. (g) O'Neill, M. E.; Wade, K. *Inorg. Chem.* **1982**, *21*, 464–466. (h) O'Neill, M. E.; Wade, K. *Polyhedron* **1983**, *2*, 963–966.

(36) (a) Evans, D. G.; Mingos, D. M. P. *J. Organomet. Chem.* **1982**, *240*, 321–327. (b) Evans, D. G.; Mingos, D. M. P. *Organometallics* **1983**, *2*, 435–447. (c) Mingos, D. M. P. *J. Chem. Soc., Chem. Commun.* **1983**, 706–708. (d) Mingos, D. M. P. *Acc. Chem. Res.* **1984**, *17*, 311–319. (e) Mingos, D. M. P. *Inorg. Chem.* **1985**, *24*, 114–115. (f) Johnston, R. L.; Mingos, D. M. P. *J. Organomet. Chem.* **1984**, *280*, 407–418. (g) Johnston, R. L.; Mingos, D. M. P. *J. Organomet. Chem.* **1985**, *280*, 419–428.

(37) (a) Teo, B. K. *Inorg. Chem.* **1984**, *23*, 1251–1257. (b) Teo, B. K.; Longoni, G.; Chung, F. R. K. *Inorg. Chem.* **1984**, *23*, 1257–1266. (c) Teo, B. K. *Inorg. Chem.* **1985**, *24*, 115–116. (d) Teo, B. K. *Inorg. Chem.* **1985**, *24*, 1627–1638.

(38) Mingos[36c] initially reported that if a face-condensed polyhedron is made up from deltahedra A and B which have six or more vertices, the total polyhedral skeletal electron count, c, can be predicted by use of the formula $c = a + b - 50$, where a and b are the electron counts of the A and B deltahedra. The electron count of 122 predicted for the cofacial bioctahedron agrees with the actual electron count found for the Rh_9 core in the $[Rh_9(CO)_{19}]^{3-}$ trianion (**3**). However, an application of this formula to the face-condensed trioctahedral Rh_{12} core found in $Rh_{12}H_2(CO)_{25}$ leads to a prediction of 158 electrons vs. an observed electron count of 160. The utilization of the Mingos general formula ($c = a + b - 48$)[36d,g] for these cases of face-condensed bioctahedral Rh_9 and trioctahedral Rh_{12} cores gives rise to electron counts of 124 and 162, respectively, in agreement with the predicted values obtained from the Teo electron-counting model.[37b]

(39) The three-layer hcp $[Ni_{12}(CO)_{21}]^{4-}$ tetraanion[20] can be conceptually converted into a face-sharing bi(trigonal-antiprismatic) $[Ni_9(CO)_{18}]^{4-}$ tetraanion by use of the isolobal analogy.[40] This formal interconversion, which involves the partitioning of three $Ni(CO)_2$ fragments from the central $Ni_6(CO)_9$ layer of the $[Ni_{12}(CO)_{21}]^{4-}$ tetraanion and replacement by three isolobal carbonyl ligands,[40] gives rise to the *nonexistent* $[Ni_9(CO)_{18}]^{4-}$ tetraanion which has an electron count of 130 vs. a predicted value for a face-fused bi(trigonal antiprism) of only 124 (based upon the Mingos rules[36] and the Teo model[37]). This difference between the predicted and observed electron counts indicates that the construction of a hypothetical species by application of the isolobal analogy must be viewed with caution, especially without an MO treatment to determine whether the added electrons would have to be accommodated in antibonding MO's.

(40) Underwood, D. J.; Hoffmann, R.; Tatsumi, K.; Nakamura, A.; Yamamoto, Y. *J. Am. Chem. Soc.* **1985**, *107*, 5968–5980 and references cited therein.

(41) Slovokhotov and Struchkov[42] proposed in 1983 that the Wade rule[35] of $2n + 2$ polyhedral skeletal electrons for a closo-n-vertex deltahedral cluster can be extended to a bis-n-vertex conjuncto polyhedron composed of two condensed deltahedra. It is intriguing that this modification (that vertices common to adjacent polyhedra are excluded from the total number of cluster vertices) leads to a predicted value of 14 skeletal electrons for the $[Rh_9(CO)_{19}]^{3-}$ trianion in agreement with the observed value.

(42) Slovokhotov, Yu. L.; Struchkov, Yu. T. *J. Organomet. Chem.* **1983**, *258*, 47–51.

(43) Mealli, C. *J. Am. Chem. Soc.* **1985**, *107*, 2245–2253 and references cited therein.

(44) (a) King, R. B. *Inorg. Chim. Acta* **1982**, *57*, 79–86. (b) King, R. B.; Rouvray, D. H. *J. Am. Chem. Soc.* **1977**, *99*, 7834–7840. (c) King, R. B. In *Chemical Applications of Topology and Graph Theory*; King, R. B., Ed.; Elsevier: Amsterdam, 1983; pp 99–123. (d) King, R. B. *Molecular Structures and Energetics*; Liebmen, J. F., Greenberg, A., Eds.; Chapter 1 for Vol. 2, pp 1–35.

(45) King, R. B. In *The Applications of Mathematical Concepts to Chemistry*; N. Trinajstic, No., Ed.; Ellic Horwood: Chichester, in press. King, R. B. *Inorg. Chim. Acta*, in press.

(46) The King model[45] for the Pt_9 core of **2** is based upon the premises that (1) each $Pt(CO)_2$ vertex uses four internal orbitals, rather than the normal three, such that each $Pt(CO)_2$ donates four skeletal electrons, (2) each vertex of degree four for the interior Pt_3 triangle matches the four internal orbitals in accordance with expectations for edge-localized bonding, and (3) each vertex of degree three for the two external Pt_3 triangles utilizes three of the four internal orbitals for edge-localized bonding. The remaining one internal orbital on each external vertex is designated as a Möbius orbital; the three such orbitals at each external Pt_3 triangle combine to give a twisted ring of *two* bonding MO's which accommodate two delocalized skeletal electrons pairs. Hence, the 38 skeletal electrons obtained from the nine Pt atoms and 2– charge are utilized in forming 15 edge-localized electron-pair bonds and delocalized Möbius bonds involving two electron pairs at each external Pt_3 triangle.

(47) The tensor surface harmonic theory developed by Stone[48] provides a highly useful guide for a comprehensive understanding of the electron-counting rules for metal clusters. The qualitative theory has been modified by Fowler and Porterfield[49] to produce a practical scheme for calculations of the extended Hückel type.

(48) (a) Stone, A. *J. Mol. Phys.* **1980**, *41*, 1339–1354. (b) Stone, A. J. *Inorg. Chem.* **1981**, *20*, 563–571. (c) Stone, A. J.; Alderton, M. J. *Inorg. Chem.* **1982**, *21*, 2297–2302. (d) Stone, A. J. *Polyhedron* **1984**, *3*, 1299–1306.

(49) Fowler, P. W.; Porterfield, W. W. *Inorg. Chem.* **1985**, *24*, 3511–3518.

(50) Johnston and Mingos[36f] have applied the Stone TSH theory[48] to demonstrate how the MO's of three-connected (electron precise) polyhedra (e.g., a trigonal prism) differ from those of corresponding deltahedral polyhedra (e.g., a trigonal antiprism or octahedron).

(51) In this connection, Woolley[52] recently emphasized that the isolobal principle and electron-counting rules are symmetry-based whereas the energetics and details of the electronic structure of transition-metal clusters are a separate matter requiring appropriate methods of theoretical analysis.

(52) Woolley, R. G. *Inorg. Chem.* **1985**, *24*, 3525–3532.

description[13] proposed in 1971 for the $[M_2Ni_3(CO)_{16}]^{2-}$ dianions suggested normal electron-pair Ni–Ni interactions within the central $Ni_3(CO)_3(\mu\text{-}CO)_3$ fragment and delocalized, multicentered metal–metal interactions involving the trinickel fragment and the two apical $M(CO)_5$ moieties.

During the last 8 years, a number of theoretical calculations have been carried out on the $[M_3(CO)_3(\mu\text{-}CO)_3]_n^{0,2-}$ monomers (n = 1)[32,40,43,53-57] and dimers (n = 2)[40,54,55b,56,57] of nickel and platinum and on the platinum trimer (n = 3).[56,57] Several important bonding features for these oligomers have emerged from these analyses. Extended Hückel calculations,[32,40,43,53,57] INDO calculations,[55] and chemical pseudopotential calculations[54,56] have established that the intraplanar stability of the $M_3(CO)_3(\mu\text{-}CO)_3$ monomers expectedly arises from strong interactions between the bridging carbonyl ligands and the metal framework and not from direct metal–metal bonding interactions. However, Mealli[43] concluded that Pt–Pt single bonds must be operative in the $Pt_3(CO)_6$ monomer in order to attain a 16-electron configuration at each planarly coordinated metal; Mealli[43] also emphasized the contribution of the metal d AO's in the M_3 bonding. Most of these theoretical treatments[32,40,43,53,56,57] also showed for the D_{3h} $[M_3(CO)_3(\mu\text{-}CO)_3]^{2-}$ monomers that the HOMO containing the extra two electrons (due to the 2– charge) is an a_2'' MO composed mainly of out-of-plane carbonyl π^* orbitals together with a lesser degree of out-of-plane metal p_z AO's. Since the HOMO's for the nickel and/or platinum dimers and platinum trimer were also found from calculations to be the in-phase a_1' bonding combinations of the a_2'' HOMO for the monomers, it was suggested[40,53,56,57] that the extra two electrons in the delocalized HOMO's provide the stabilization energy or "glue" for holding the interlayers together. Hoffmann and co-workers[40] showed that an out-of-plane bending of the carbonyl ligands by 15° in the nickel dimer not only minimized interlayer steric interactions but also stabilized the HOMO by increased electron density on the metal atoms and by a hybridization with metal valence s, p_z, and d_{yz} AO's to give stronger bonding due to better orbital overlap. Hence, the interlayer bonding in the nickel and platinum dimers is a composite of three contributions: (1) intertriangular metal–metal interactions; (2) direct carbonyl–carbonyl bonding interactions involving interlayer carbonyl π^* MO's; and (3) metal–carbonyl interactions involving interlayer metal orbitals and carbonyl π^* MO's for carbonyl ligands not directly coordinated to the metal atoms.[55]

Bullett,[56] Hoffmann,[40] and Mingos[57] pointed out that stabilization of the HOMO for a $[M_3(CO)_6]_n^{2-}$ dianion will be greater for an eclipsed D_{3h} conformation (as in the platinum dimer) where the corresponding interlayer carbonyl ligands lie directly over each other. This effect is counterbalanced by a reduction of steric interactions for the staggered D_{3d} conformation, for which a smaller interplanar distance would favor stronger metal–metal interactions. It was concluded[40,56,57] that the observed different conformations for the nickel and platinum dimers reflect the larger size of the platinum atom and its inherently greater tendency to form stronger metal–metal interactions at a larger internuclear separation.

These MO treatments indicate that the stability of the $[M_3(CO)_6]_n^{2-}$ oligomers is caused more by bonding carbonyl–carbonyl interactions (which are optimized for a D_{3h} geometry) than metal–metal interactions.[58] This conclusion[40,56,57] is compatible with both the X-ray photoemission spectra[33] and with the ^{195}Pt and ^{13}C NMR spectra[34] of the $[Pt_3(CO)_6]_n^{2-}$ series (n = 2–5).

The observation[34] that ^{13}C NMR spectra of the $[Pt_3(CO)_6]_n^{2-}$ dianions (n = 2–4) show unambiguously that the bridging and terminal carbonyls retain their identity (i.e., do not intraexchange) is in accordance with calculations by Mealli[43] on the planar $Pt_3(CO)_3(\mu\text{-}CO)_3$ fragment indicating a considerable rotational barrier to interconversion. In contrast, an interconversion of the bridging and terminal carbonyl ligands in the $[Ni_6(CO)_{12}]^{2-}$ dianion was proposed[34b] on the basis of a room-temperature ^{13}C NMR spectrum showing only one broad line. This fluxional behavior may be ascribed to a concerted motion[59] of all carbonyl ligands about the pseudo threefold axis relative to the Ni_6 core.

An extension of this bonding model to 1 supports the premise that its observed hybrid conformation must be a compromise between electronic and steric effects. It also follows that 1 should be more unstable than the $[Ni_6(CO)_{12}]^{2-}$ dianion, as indicated from its facile reaction with halide ions to yield the $[Ni_6(CO)_{12}]^{2-}$ dianion along with decomposition products.[7]

Acknowledgment. This research was supported by the National Science Foundation (CHE83-15312). We thank Professor Bruce King (Department of Chemistry, University of Georgia) for providing us with a preprint of his article "Metal Cluster Topology: Application to Gold and Platinum Clusters" (presented at an International Symposium on Applications of Mathematical Concepts to Chemistry in Dubrovnik, Yugoslavia, 1985). D.A.N. wishes to thank Professor June L. Dahl for her helpful suggestions in the preparation of the paper.

Registry No. $[AsPh_4]_2^+[1]$, 60512-60-9; $[NBu_4]_2^+[Ni_6(CO)_{12}]^{2-}$, 93756-04-8.

Supplementary Material Available: Tables of atomic coordinates and isotropic thermal parameters for the two independent monocations, anisotropic thermal parameters for all non-hydrogen atoms, bond angles for the $[Ni_9(CO)_{18}]^{2-}$ dianion, and interatomic distances and bond angles for the two independent $[AsPh_4]^+$ monocations (9 pages); a listing of observed and calculated structure factor amplitudes for $[AsPh_4]^+_2$ $[Ni_9(CO)_{18}]^{2-}$ (29 pages). Ordering information is given on any current masthead page.

(53) Evans, J. *J. Chem. Soc., Dalton Trans.* **1980**, 1005–1011.
(54) Chang, K. W.; Woolley, R. G. *J. Phys. C.: Solid State Phys.* **1979**, *12*, 2745–2768.
(55) (a) Pacchioni, G.; Fantucci, P.; Valenti, V. *J. Organomet. Chem.* **1982**, *224*, 89–105. (b) Fantucci, P.; Pacchioni, G.; Valenti, V. *Inorg. Chem.* **1984**, *23*, 247–253.
(56) Bullett, D. W. *Chem. Phys. Lett.* **1985**, *115*, 450–453.
(57) McEvoy, N. A.; Evans, D. G.; Mingos, D. M. P., unpublished results. Cited in ref 15 of paper by Hoffmann and co-workers.[40]

(58) Aside from this conclusion concerning the relative importance of interlayer carbonyl–carbonyl bonding interactions in stabilizing the nickel and platinum oligomers, the bonding model resulting from the extended Hückel and chemical pseudopotential calculations[40,56,57] bears a marked similarity to the qualitative MO scheme initially proposed[13] 15 years ago for the $[M_2Ni_3(CO)_{16}]^{2-}$ dianions (M = Mo, W) and subsequently applied[8] to the $[Ni_5(CO)_{12}]^{2-}$ dianion. It is noteworthy that this model (involving localized electron-pair Ni–Ni bonds within the $Ni_3(CO)_3(\mu\text{-}CO)_3$ plane and delocalized, multicentered electron-pair bonding between the central Ni_3 triangle and two apical $M(CO)_5$ or $Ni(CO)_3$ groups) does not agree with the results of INDO calculations[55] on both the neutral and doubly charged $[Ni_5(CO)_{12}]^{0,2-}$ and $[Ni_6(CO)_{12}]^{0,2-}$ clusters. These calculations[55] showed for both the Ni_5 and Ni_6 clusters that direct Ni–Ni interactions within the $Ni_3(CO)_3(\mu\text{-}CO)_3$ layers have repulsive character while the out-of-plane Ni–Ni interactions are of bonding character (with considerably stronger Ni–Ni bonds in the Ni_5 cluster). This prediction of repulsive interactions between pairs of intratriangular nickel atoms separated by short Ni–Ni distances (2.36 Å) and attractive interactions between in-plane and out-of-plane nickel atoms separated by much longer Ni–Ni distances (2.8 Å) is surprising. Moreover, the fact that the INDO calculations[55] predict that the neutral forms of the Ni_5 and Ni_6 clusters are more stable than the corresponding anionic forms (in contradistinction to the extended Hückel and chemical pseudopotential calculations[40,43,56,57]) casts considerable doubt on the validity of the results.
(59) Johnson, B. F. G. *J. Chem. Soc., Chem. Commun.* **1976**, 703–704.